

# Preparation of TiO<sub>2</sub>@SiO<sub>2</sub> with a Hollow Olive-shaped Cable by Electrospinning

Qian Feng<sup>a</sup>, Lei Wang<sup>\*a</sup>, Liye Su<sup>a</sup>, Shuzhi Xu<sup>b</sup>

<sup>a</sup>North China University of Science and Technology, Tangshan 063210, China

<sup>b</sup>School of Grain, Jilin Business and Technology College, Changchun 130507, China  
wdl8898@yeah.net

The TiO<sub>2</sub>@SiO<sub>2</sub> coaxial hollow olive-shaped cable has been prepared by using the three-layer coaxial electrospinning technique. This technique also can be used to prepare the coaxial olive-shaped cable of other inorganic substances. In this paper the samples were characterized adopting many-ways such as differential thermal analysis (TG-DTA) and X-ray diffractometry (XRD), infrared spectrograph (FTIR), scanning electron microscopy (SEM), transmission electron microscopy (TEM) and energy dispersive spectrometer (EDS) techniques. XRD analysis and FTIR analysis show that the coaxial hollow olive-shaped cable obtained at 600°C has an inner wall of crystalline TiO<sub>2</sub> and an outer wall of amorphous SiO<sub>2</sub>. SEM analysis and TEM analysis show that the coaxial hollow olive-shaped cable is formed after sintering at 600°C. Its middle diameter is about 1.4 μm, the terminal diameter is about 210 nm, the thickness of the inner wall is about 200 nm, the shell thickness is about 100 nm and the length of the shell is about 5 μm. However, after sintering at 800°C, the olive-shaped hollow tube collapses. EDS analysis shows that the sintered samples mainly contain three elements which are O, Si and Ti. The formation mechanism of the TiO<sub>2</sub>@SiO<sub>2</sub> hollow olive-shaped cables is preliminarily investigated.

## 1. Introduction

One-dimensional nanomaterials, such as nanowires, nanotubes, nanobelts and nanocables, have been successfully synthesized by many methods. In recent years, researchers have paid great attention to the synthesis of multilayer coaxial composite nanomaterials. For example, DG Shin and others synthesized the MoS<sub>2</sub>/CNT coaxial nanotube by using hydrothermal method (Shin, et al., 2015); Hu and others combined the thermal precipitation and physical evaporation to synthesize three-layer coaxial nanocables (Ga/Ga<sub>2</sub>O<sub>3</sub>/ZnO) and the Ga<sub>2</sub>O<sub>3</sub>/ZnO two-layer coaxial nanotubes (Hu, et al., 2014); for the composite material of one-dimensional TiO<sub>2</sub>/SiO<sub>2</sub> nano-structured materials, Zhang and others prepared the coaxial TiO<sub>2</sub>/SiO<sub>2</sub> nanotubes by using the sol-gel and gas method; Xu and others prepared the TiO<sub>2</sub>/SiO<sub>2</sub> composite hollow nanofibres, TiO<sub>2</sub>@SiO<sub>2</sub> submicron coaxial cables and TiO<sub>2</sub>@SiO<sub>2</sub> coaxial double-wall submicron by using electrospinning technology (Xu, et al., 2012).

In this paper, electrostatic spinning is carried out by replacing a single nozzle with three-layer coaxial nozzles, and after one step, TiO<sub>2</sub>@SiO<sub>2</sub> hollow olive-shaped cables are prepared directly. The samples are characterized by using modern analytical techniques, and their formation mechanism is analyzed, thus, some meaningful results are obtained.

## 2. Experimental

### 2.1 Preparation of precursor solution

A certain amount of polyvinylpyrrolidone (PVP, average molecular weight is 1300000, AR) is added to the mixed solution of the appropriate amount of anhydrous ethanol (C<sub>2</sub>H<sub>5</sub>OH, AR) and chloroform (CHCl<sub>3</sub>, AR). After magnetic stirring at room temperature for 3h, a certain amount of ethyl orthosilicate [(C<sub>2</sub>H<sub>5</sub>O)<sub>4</sub>Si, AR] is added to it, and then it continues to be magnetically stirred for 6h. After that, it should stay for 3h and then

the outer spinning solution [PVP + (C<sub>2</sub>H<sub>5</sub>O) 4Si + C<sub>2</sub>H<sub>5</sub>OH + CHCl<sub>3</sub>] can be obtained. The mass fraction of PVP, (C<sub>2</sub>H<sub>5</sub>O) 4Si, C<sub>2</sub>H<sub>5</sub>OH and CHCl<sub>3</sub> is respectively the 8.0%, 14.7%, 61.7% and 15.6%.

After the mixed solution (volume ratio is 1:1) of sesame oil and sorbitan oleate (Span-80 emulgator) is stirred at room temperature for 3h, the butyl titanate with equal volume is added to it, and then it continues to be stirred for 6h. After that, it should stay for 3h and then the interlayer spinning solution [Sesame oil+Span-80+Ti(OC<sub>4</sub>H<sub>9</sub>)<sub>4</sub>] can be obtained. The mass fraction of butyl titanate, sesame oil and sorbitan oleate is respectively the 50.1%, 23.9% and 26.0%.

## 2.2 The preparation of [Sesame oil+Span-80+ Ti(OC<sub>4</sub>H<sub>9</sub>)<sub>4</sub>]@ [PVP+ (C<sub>2</sub>H<sub>5</sub>O) 4Si] coaxial hollow composite fiber

Three-layer coaxial electrostatic spinning device is shown in Figure 1. The three-layer coaxial nozzle is composed of three stainless steel tubes that all nest inside one another, and the inner diameters of the inner, middle and outer nozzles are respectively the 0.7mm, 1.2 mm and 1.8 mm. The inner nozzle is about 0.5mm shorter than the middle nozzle, and also the middle nozzle is about 0.5mm shorter than the outer nozzle. Each spray tube is respectively connected with the inner, middle and external liquid storage containers. Make sure the spray tubes are coaxial and the gap can flow smoothly out of the solution.

The prepared [PVP + (C<sub>2</sub>H<sub>5</sub>O) 4Si + C<sub>2</sub>H<sub>5</sub>OH + CHCl<sub>3</sub>] solution, as the outer solution, is placed in the external liquid storage container. The [Sesame oil+Span-80+ Ti(OC<sub>4</sub>H<sub>9</sub>)<sub>4</sub>] solution, as the intermediate solution is placed in the middle liquid storage container. The inner liquid storage container is connected with the atmosphere. The DC positive electric field is directly added to the outer layer and the intermediate layer solution, and the spinning formed [Sesame oil+Span-80+Ti(OC<sub>4</sub>H<sub>9</sub>)<sub>4</sub>]@ [PVP+(C<sub>2</sub>H<sub>5</sub>O) 4Si] coaxial composite fibers are received by the aluminum foil which connects with the negative electrode. In the experiment, the distance between the nozzle and the receiving screen is 12cm, the applied voltage is 7.0kV, the ambient temperature is 18-20°C, and the environmental humidity is 40%-45%.

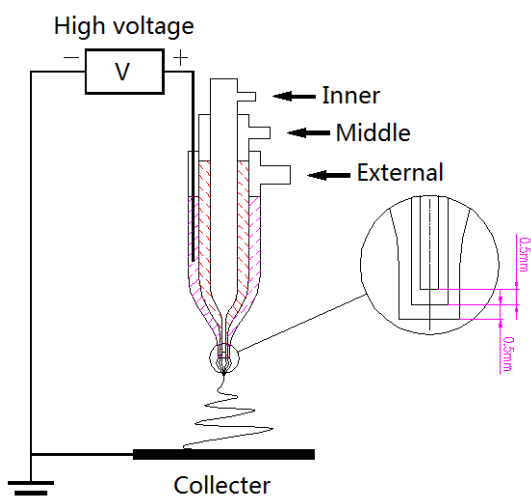


Figure 1: Setup of the multilayer coaxial electrospinning

## 2.3 The preparation of the TiO<sub>2</sub>@SiO<sub>2</sub> hollow olive-shaped cable

The prepared [Sesame oil+Span-80+ Ti(OC<sub>4</sub>H<sub>9</sub>)<sub>4</sub>]@ [PVP+ (C<sub>2</sub>H<sub>5</sub>O) 4Si] coaxial composite fibers are roasted through the programmed temperature control furnace, and the heating rate is 1°C/min. When the temperature is 600 °C and 800 °C, after keeping the constant temperature for 10 h, the temperature should be reduced to the room temperature at the same rate, and then the TiO<sub>2</sub>@SiO<sub>2</sub> hollow olive-shaped cable can be obtained.

## 2.4 Characterization method

Y-2000 X-ray diffractometer produced by Shengda Ray Instrument Co., Ltd is used to make the structural analysis. Cu target K $\alpha$  radiation is used, Ni is taken as the filter, the scanning speed is 3°/min, step size is 0.04°, working current is 20 mA and voltage is 40kV. The XL-30 field emission environment scanning electron microscope of Netherlands PHILIPS Company is used to analyze the diameter and morphology of the fiber. JEM-2010 transmission electron microscope of Japanese JEOL Company is used to analyze the fiber

structure. OXFORD ISIS-300 X-ray energy dispersive spectrometer is used to make the elemental analysis. The FTIR8400S FTIR spectrometer of Japanese Shimadzu Company is used to make the FTIR analysis of the sample. KBr squash technique is used and the wave-number range is 4000-400cm<sup>-1</sup>.

### 3. Results and discussion

#### 3.1 XRD Analysis

Figure 2 is the XRD diagram of the sample after the sintering of the composite fiber for 10 h at 600°C(a) and 800°C(b). We can see that with the increase of sintering temperature, the organic matter is gradually oxidized and decomposed, and also volatilizes from Figure 2(a). And the broad amorphous dispersion peak appears, which is mainly the diffraction peak of amorphous SiO<sub>2</sub>. When  $2\theta = 25.281^\circ(101)$ ,  $36.946^\circ(103)$ ,  $37.800^\circ(004)$ ,  $38.575^\circ(112)$  and  $48.049^\circ(200)$ , the weak diffraction peaks of anatase TiO<sub>2</sub> appear. Their d value and the relative intensities are basically the same as the d value and relative intensities listed in PDF card (21-1272) of TiO<sub>2</sub>. At the same time, when  $2\theta = 27.446^\circ(110)$ ,  $36.085^\circ(101)$ ,  $54.322^\circ(211)$  and  $56.640^\circ(220)$ , the weak diffraction peaks of rutile TiO<sub>2</sub> appear, indicating that TiO<sub>2</sub> is the mixed crystal crystalline form of anatase and rutile at 600 °C. When the sintering temperature reaches 800°C, from the Figure 2(b), we can see that the broad amorphous dispersion peak around  $2\theta = 22^\circ$  is mainly the diffraction peak of amorphous SiO<sub>2</sub>. The diffraction peak of anatase TiO<sub>2</sub> weakens, but the characteristic diffraction peak of the rutile crystal face strengthens. When  $2\theta = 41.225^\circ(111)$  and  $69.008^\circ(301)$ , the characteristic diffraction peaks of the rutile TiO<sub>2</sub> also appear. Their d value and the relative intensities are basically the same as the d value and relative intensities listed in PDF card (21-1276) of TiO<sub>2</sub>, indicating that when the temperature is 800°C, TiO<sub>2</sub> is mainly the rutile TiO<sub>2</sub>. The anatase TiO<sub>2</sub> and rutile TiO<sub>2</sub> both belong to the tetragonal system, and the space group is P42/mnm. Because of the cladding of shell SiO<sub>2</sub> and the influence of bonding between them, the intensity of diffraction peak of TiO<sub>2</sub> is obviously weakened.

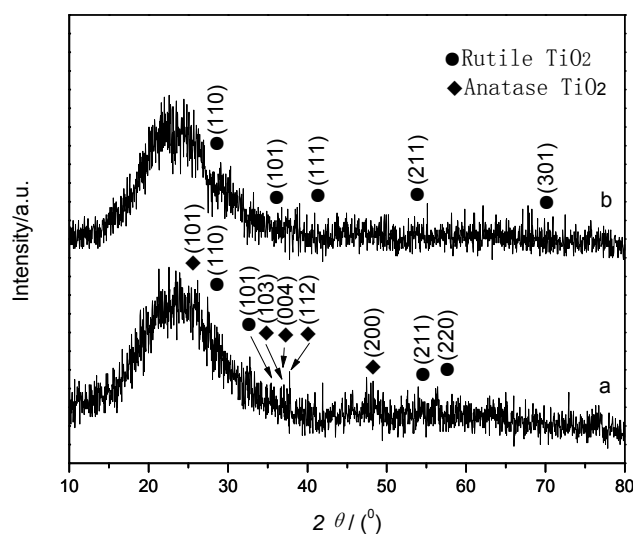


Figure 2: XRD patterns of the sample calcined at a) 600 °C and b) 800 °C for 10 h

#### 3.2 SEM Analysis

The SEM photos of sample are shown in Figure 3. We can see that at different calcination temperatures, the morphology of the sample is significantly different. From Figure 3(a) and 3(b), we can see that when sintering temperature is 600°C, the uniform hollow olive-shaped cables are mainly formed, and meanwhile some nanotubes are formed. The samples have the uniform appearance, smooth surface and no cohesiveness, and have good dispersibility. From the cross section of the sample in the figure, we can see that it presents the obvious hollow structure, the middle diameter of the olive-shaped hollow tube is between 950-2200nm, the terminal diameter of the olive-shaped hollow tube is between 100-300nm and the length is between 4-8 $\mu$ m. Due to the different fracture position of the fibers, at the same time some nanotubes are formed. The diameter of the nanotubes is between 500-700nm and the length is between 2-6 $\mu$ m. From the Figure 3(c) and 3(d), we can see that with the increase of sintering temperature, when the sintering temperature is 800°C, the olive-shaped hollow tube collapses because the wall of the formed hollow tube is thin, the volume of the hollow part increases and the surface tension of the tube is not enough to support the hollow structure of the tube.

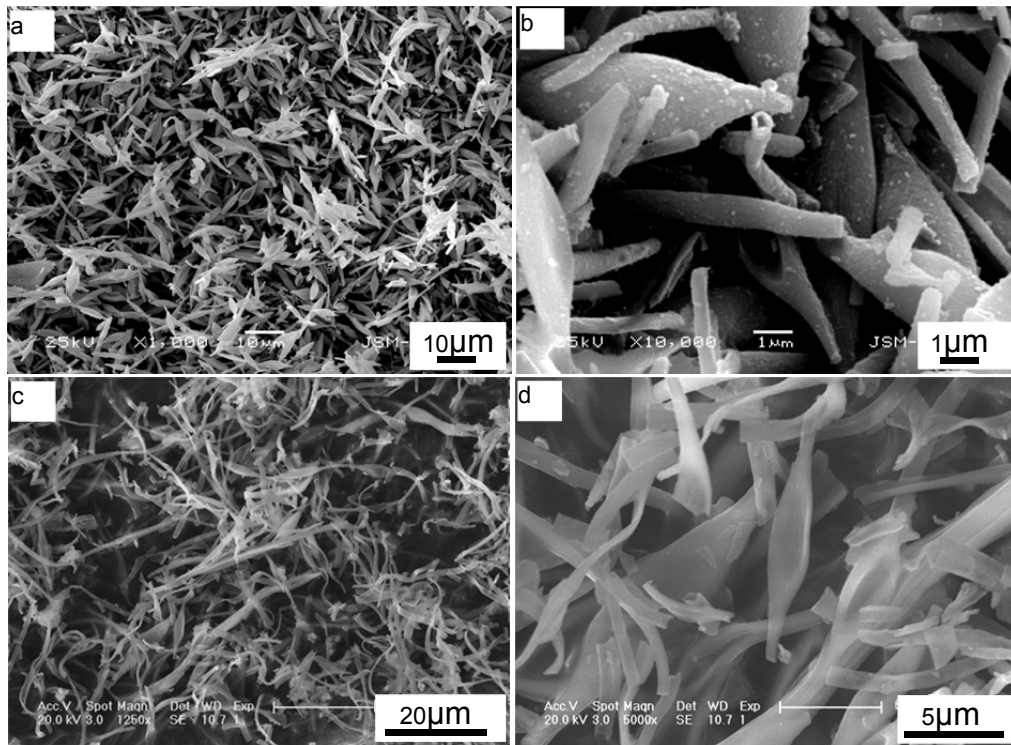


Figure 3: SEM images of samples at a-b) 600 °C and c-d) 800 °C

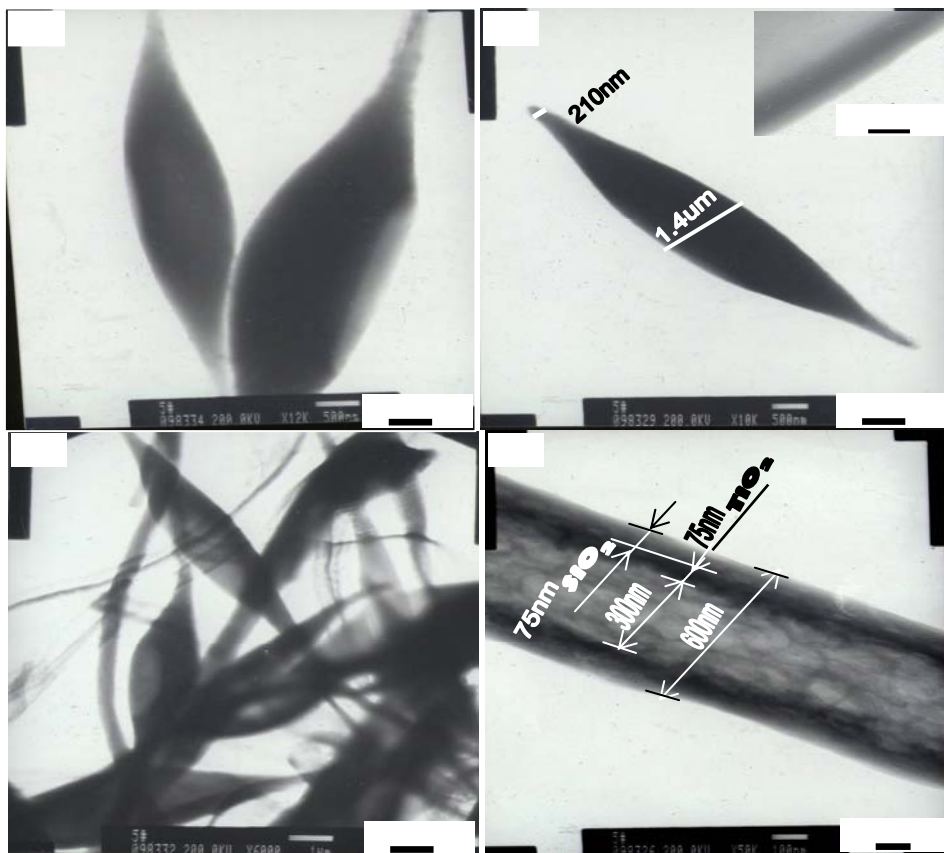


Figure 4: TEM images of samples at 600 °C

### 3.3 TEM Analysis

TEM is used to further make the structural analysis. The transmission electron microscope images of the samples when the sintering temperature is 600°C are shown in Figure 4, and the olive-shaped hollow tube is formed. Figure 4(b) is a TEM photo of a single olive-shaped hollow tube with good coaxiality and uniform radial distribution. The middle diameter of the olive-shaped hollow tube is about 1.4  $\mu\text{m}$  and the terminal diameter is about 210nm. The figure 4(b) illustration is the local high resolution TEM photo. The light color of the contrast of the core shows that the core is hollow. Due to differences in property and the structure of the matrix material, the tube wall presents the obvious stratification, which shows that the inner wall of the tube and the shell have different chemical compositions, and the olive-shaped hollow tube is a multi-walled structure. The thickness of the inner wall is about 200nm, the thickness of the shell is about 100nm and the length is about 5 $\mu\text{m}$ . Figure 4(d) is the TEM photo of the tubular portion. It is the hollow structure, the tube wall is obviously stratified and typical multi-walled nanotube is formed. The diameter of the nanotube is about 600nm, the diameter of the hollow part of the core is about 300nm, and the thickness of the inner wall of the tube and the shell is about 75nm. The flocculation material on the fiber surface is amorphous  $\text{SiO}_2$ , and the particles are crystalline  $\text{TiO}_2$  particles.

### 3.4 FTIR analysis

Figure 5 is the infrared spectrogram of the sample after sintering to 600°C(a) and 800°C (b).

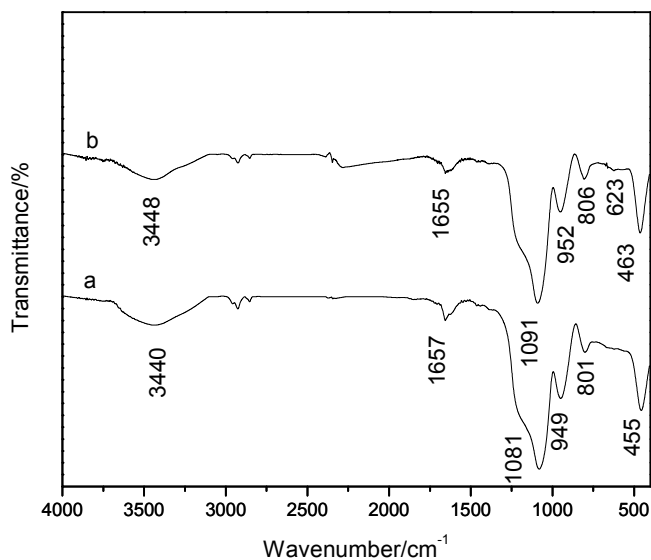


Figure 5: FTIR spectra of the samples at a) 600°C and b) 800°C

According to the figure, we can see that after sintering to 600°C and 800°C, the spectrograms were basically the same, indicating that the sample gets the pure inorganic ingredients. From figure 5 (b), we can see that absorption peak at 952  $\text{cm}^{-1}$  is caused by the vibration of Si-O-Ti bond, which shows that the new chemical bonds are formed among Ti, O and Si. The absorption peaks at 806 $\text{cm}^{-1}$  and 463 $\text{cm}^{-1}$  are the bending vibration absorption of Si-O-Si bond. The intensity of the vibration absorption peak of Ti-O bond at 623 $\text{cm}^{-1}$  is weak, which is mainly caused by the cladding of the shell  $\text{SiO}_2$ . The absorption peaks at 1091 $\text{cm}^{-1}$  and 806 $\text{cm}^{-1}$  are the vibrations of the Si-O bond. The hydroxyl absorption peak at 3448 $\text{cm}^{-1}$  is relatively sharp, indicating that the surface of it contains a large number of Si-OH radical groups. The hydroxyl association absorption peak at 1655 $\text{cm}^{-1}$  shows that there is a strong adsorption between fibers.

### 3.5 EDS analysis

In order to further determine the composition of the generated olive-shaped cable, the EDS analysis has been made for the sample (800°C), as shown in Figure 6. We can observe the spectral peak of the O, Si and Ti (Au and C come from the metal spraying of the sample surface before test, and the sample's double faced adhesive tape or underfiring residue before the test), which shows that the sample contains three kinds of elements which are O, Si and Ti.

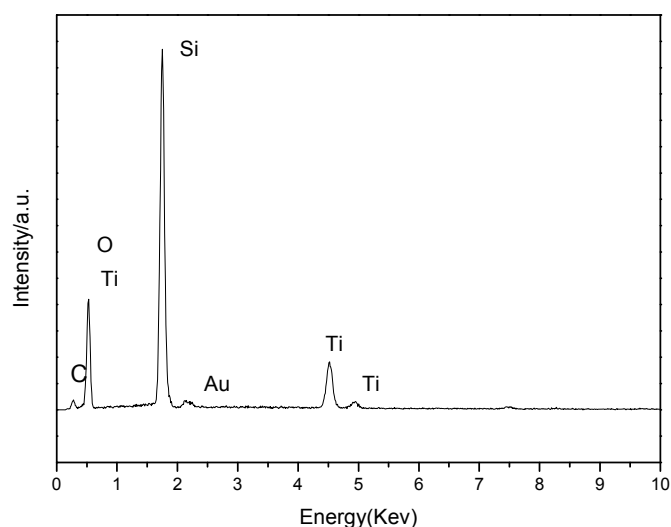


Figure 6: EDS surface analysis of samples calcined at 800 °C

#### 4. Conclusions

TiO<sub>2</sub>@SiO<sub>2</sub> hollow olive-shaped cables were successfully synthesized by coaxial electrospinning technique using tetrabutyl titanate, tetraethyl orthosilicate, polyvinyl pyrrolidone, absolute ethanol, sesame oil, span-80 and chloroform as starting materials. The synthetic steps are few and the conditions are easy to control. The results indicated that the products are TiO<sub>2</sub>@SiO<sub>2</sub> hollow olive-shaped cables with an amorphous SiO<sub>2</sub> outer shell, a crystalline TiO<sub>2</sub> inwall. The hollow olive-shaped cables possess thickness of inwall of ca. 200 nm and outer shell of ca. 100 nm, medi-diameter of ca. 1.4 μm, erminal diameter of ca. 210 nm, length of ca. 5 μm.

#### Acknowledgments

This work is supported by the Science and Technology Program Project of Hebei Province (No. 16271603).

#### Reference

- Hu T., LQ Ye, WL Li, JH Luo, B Jiang, 2014, Preparation and characterization of TiO<sub>2</sub>-SiO<sub>2</sub>/TiO<sub>2</sub> two-layer antireflective coating photo-catalyst, Chinese Journal of Inorganic Chemistry, 30(8), 1778-1782.
- Shin DG, EJ Jin, YJ Lee, WT Kwon, Y Kim, 2015, TiO<sub>2</sub>-SiO<sub>2</sub> Nanocomposite Fibers Prepared by Electrospinning of Ti-PCS Mixed Solution, Korean Chemical Engineering Research, 53(3), 276-281.
- Xu Sz, XT Dong, GQ Gai, JX Wang, GX Liu, TX Lu, 2012, Preparation of TiO<sub>2</sub>@SiO<sub>2</sub> coaxial double-walled submicrotubes by trifluidic coaxial electrospinning and its photocatalytic property, Acta Chimica Sinica, 70(15) :1660-1666.
- Zhang Sh, XT Dong, SZ Xu, JX Wang, 2008, Preparation and characterization of TiO<sub>2</sub>/SiO<sub>2</sub> composite hollow nanofibres via an electrospinning technique, Acta Materiae Compositae Sinica, 25 (3):138-143.